Thin Solid Films 519 (2011) 6319–6322

Contents lists available at ScienceDirect

Thin Solid Films

journal homepage: www.elsevier.com/locate/tsf

Oxygen vacancy in Al_2O_3: Photoluminescence study and first-principle simulation

V.A. Pustovarov [a], T.V. Perevalov [b], V.A. Gritsenko [b], T.P. Smirnova [c,*], A.P. Yelisseyev [d]

[a] Ural State Technical University, 19 Mira St. 620002, Ekaterinburg, Russia
[b] Institute of Semiconductor Physics, 13 ak. Lavrentiev ave. 630090, Novosibirsk, Russia
[c] Institute of Inorganic Chemistry, 3 ak. Lavrentiev ave. 630090, Novosibirsk, Russia
[d] Institute of Geology and Mineralogy, 3 ak. Koptyug ave., 630090, Novosibirsk, Russia

ARTICLE INFO

Article history:
Received 12 October 2010
Received in revised form 1 April 2011
Accepted 5 April 2011
Available online 13 April 2011

Keywords:
Alumina
Thin films
Density functional theory
Simulation
Photoluminescence
Chemical vapor deposition

ABSTRACT

Broad photoluminescence (PL) band at 2.97 eV excited in the band near 6.0 eV in amorphous chemical vapor deposition films is related to the neutral oxygen vacancy by analogy with crystalline Al_2O_3. The identification of this PL band was supported by the results of first-principle quantum chemical simulation, which showed 6.3 and 6.4 eV bands in the extinction spectra for α- and γ-Al_2O_3, respectively. Other PL bands are attributed to ionized single vacancies (F^+-centers), divacancies (F_2) and, probably, interstitial Al.

1. Introduction

The exceptional properties of alumina (Al_2O_3), such as great hardness, high thermal and chemical stability, and high melting temperature, make it a very attractive material. The crystalline α-Al_2O_3 phase (corundum or sapphire) is the single stable modification of alumina. The crystalline α-Al_2O_3 has the band gap $Eg \approx 8.5$ eV and is widely used in optical devices. Sapphire doped with chrome (ruby) or titanium is applied as an active medium in laser systems. In microelectronics sapphire is used as a substrate for growing silicon and gallium nitride (GaN). Alumina is a highly radiation-resistant material and is used as a sensitive element in detectors when measuring the ionizing radiation parameters. Formation of defects in irradiated sapphire is the subject of numerous researches [1–8].

Recently much attention has been focused on amorphous alumina (Al_2O_3) films. Alumina has a high permittivity ($\varepsilon \approx 10$) compared to silicon oxide SiO_2 ($\varepsilon = 3.9$) which was used as a gate dielectric in Metal-Oxide-Semiconductor (MOS) devices (field-effect transistors) for last five decades. The informational density of silicon integrated circuits grows with the decrease of the length of the MOS transistor channel. The reduction of channel length is accompanied also by the increase in gate capacity. Thus the gate capacity increases with decreasing the SiO_2 gate thickness. At present, typically used technology node is 63 nm. Under such conditions the thickness of thermal SiO_2 gate is 1.2 nm. Further decrease in the length of MOS transistor channels requires the increase in gate capacity. However the capacity cannot be increased at the expense of further thinning of the thermal oxide layer because of the unacceptably strong tunnel current through the dielectric layer. The heavy tunnel current results in the reduction of the steepness of current–voltage characteristics of transistor because of minority current extraction from the channel. In addition, it causes unacceptably high additional dissipation of power (heating).

The major approach to the increase in gate capacity is the replacement of thermal oxide by insulators with the high value of permittivity (the so-called high-k dielectric). Amorphous alumina can be used for this purpose [9–11]. Recently amorphous alumina is used in the development of giga-and terabits scale flash memory. Amorphous silicon nitride (Si_3N_4) with a high concentration of charge carrier traps is used as a memory medium in this flash memory cell [12,13]. Usage of amorphous Al_2O_3 allows one to increase the thickness of tunnel oxide from 2 to 5 nm. The increase of tunnel oxide thickness results in the blocking of tunnel current in the storage mode of a flash memory cell and in the increase in its reliability. However, the layer of Si_3N_4 is covered by the layer of amorphous Al_2O_3 and the charge from silicon nitride can flow down through traps in Al_2O_3. Therefore, understanding of the nature of (atomic and electronic structure) of traps in amorphous Al_2O_3 is of great interest.

The aim of this work is spectroscopic study of the photoluminescence of amorphous Al_2O_3 in comparison with the results of theoretical simulation of oxygen vacancy. To excite the luminescence of Al_2O_3, we used synchrotron radiation (SR) providing intense

* Corresponding author. Tel.: +7 383 3309410; fax: +7 383 3309489.
E-mail address: smirn@niic.nsc.ru (T.P. Smirnova).

0040-6090/$ – see front matter © 2011 Elsevier B.V. All rights reserved.
doi:10.1016/j.tsf.2011.04.014

emission in a wide spectral range from VUV to visible region. SR is a powerful tool in spectroscopic study of wide-band-gap materials, particularly crystalline and amorphous SiO_2[14–16].

2. Experimental details

2.1. Preparation of Al_2O_3 films

The Al_2O_3 films were grown in a flow-type chemical vapor deposition (CVD) reactor with hot walls using $Al(acac)_3$ (acac = pentane-2,4-dionate, $AlO_6H_3(CH_3)_6$) as precursor and argon as a carrier gas. Oxygen was supplied on a separate line. The films were deposited on the n-type Si(100) substrate with resistance ρ ~10 Ω cm. The Si substrates were cleaned by a sequence of boiling in CCl_4 and acetone. Further the substrates were etched in the $H_2SO_4 + HNO_3 = 1:1$ mixture and finally in the diluted HF (50%). The cleaning procedure resulted in removal of the native oxide and surface contaminations. The temperature of substrate was 600 °C during the CVD process. The film thickness and refractive index were determined at the single wavelength LEF-3 ellipsometer with a He–Ne laser, λ = 632.8 nm: the obtained parameters were 50–100 nm and 1.65, respectively. Photoelectron spectra were registered with VG EASCALAB HP spectrometer using nonmonochromatic Al Kα radiation with $h\nu = 1486.6$ eV, the films had been shown to consist only of aluminum and oxygen atoms and their composition is close to Al_2O_3. According to Raman scattering data, the films contain an admixture of carbon in amorphous forms, whose concentration was ~5 at.%.

X-ray diffraction measurements were carried out at the station "Anomalous scattering" of the Siberian Center of Synchrotron Radiation (λ = 1.5405 Å). Fig. 1a shows the X-ray diffraction pattern of the films, which evidences that the film is amorphous. Diffraction pattern 2 conforms to the cubic modification of γ-Al_2O_3 taken from the base of structural database (PDF-3-914). In Fig. 1b one compares the film diffraction with that of rhombohedral modification of α-Al_2O_3 (PDF-2-1227). The halo in the range from 10 to 30 of 2Θ points to amorphous structure of Al_2O_3 films, short-range order of which complies with cubic γ-Al_2O_3

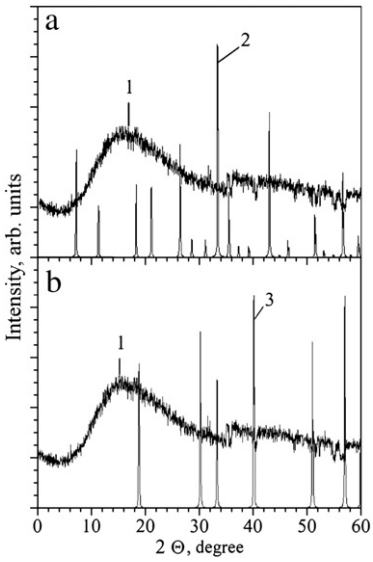

Fig. 1. X-ray diffraction patterns for amorphous Al_2O_3 films (1) and crystalline Al_2O_3 of cubic (γ-Al_2O_3, PDF-3-914, pattern 2) and rhombohedral (α-Al_2O_3, PDF-2-1227, 3) modifications.

2.2. Computational procedure

The theoretical results are obtained using the QUANTUM-ESPRESSO code [17], which implements density functional theory within the plane-wave as a basis set and pseudopotential approximation [18]. The core electrons were described using norm-conserving Local Density Approximation in the Perdew–Zunger parameterization [17]. We use a periodic supercell approach for the calculation of the oxygen vacancy in α-Al_2O_3 and γ-Al_2O_3. The Brillouin Zone of the unit cell was sampled with 2×2×2 Monkhorst–Pack k-points mesh for both α- and γ-Al_2O_3 supercells. The plane-wave cutoff energy was taken equal to 30 Ry.

The perfect crystal of α-Al_2O_3 has a trigonal unit cell containing two Al_2O_3 molecules (space group R-3cR). The coordinates of the atoms are such that an Al atom is surrounded by six O atoms of two different nearest-neighbor (NN) distances and each O atom has four NN Al atoms. The crystal structure of γ-alumina has been a long-standing issue. At present, there are two principal theoretical models of bulk γ-Al_2O_3: spinel-related structure and nonspinel structure [19]. It was ascertained that the band structures of both models are very close to each other [20].

Thereby in current investigations we take the minimal 40 atoms defective spinel structure of γ-Al_2O_3. This structure is derived from the spinel with two cation vacancies at octahedral sites that are farthest from each other [21]. This model was widely used in literature [22–24]. To calculate oxygen vacancy in Al_2O_3, a supercell of sufficient size should be used in order to avoid the possible defect–defect interaction. The α- and γ-Al_2O_3 supercells contain a total of 160 atoms, in which one of the interior O atoms is removed. The threefold coordinated O atom was removed in the case of γ-Al_2O_3.

2.3. Photoluminescence measurements

PL and photoluminescence excitation (PLE) spectra were measured at 7.5 K in stationary and time-resolved regimes, using synchrotron radiation on the SUPERLUM station of the DESYLAB laboratory (Hamburg, Germany) [25]. For excitation in the 3.7–26 eV range we used a 2 m vacuum monochromator with a 3.2 Å spectral resolution. PL emission was detected with the 0.3 m ARC Spectra Pro-308i monochromator and the R6358P Hamamatsu photomultiplier. Taking into account the luminescence kinetics, the time delay (δt) with respect of excitation pulse and time window length (Δt) were chosen. Two time windows were used: $\delta t_1 = 2.7$ ns, $\Delta t_1 = 11.8$ ns for the fast component and $\delta t_2 = 60$ ns, $\Delta t_2 = 92$ ns, for the slow component. The PLE spectra were measured at excitation energy normalized to an equal number of incident photons, using sodium salicylate whose quantum efficiency is independent of photon energy at $h\nu > 3.7$ eV.

3. Results and discussion

3.1. Calculation of oxygen vacancy

The peak at 6 eV was related to oxygen vacancy in [1–8]. To theoretically support this interpretation, we studied the dispersion of extinction coefficient (k) for α-Al_2O_3 and γ-Al_2O_3 in a wide range of spectra. The calculated spectra $k = f(h\nu)$ for ideal α-Al_2O_3 and γ-Al_2O_3 crystals and for these crystals with oxygen vacancies are shown in Fig. 2. To calibrate the calculation procedure, we compared the results of calculation for bulk α-Al_2O_3 with corresponding spectra from [26]. The results agree well. It is necessary to note that the calculated coefficients $k(h\nu)$ for the α-Al_2O_3 and γ-Al_2O_3 modifications have a weak anisotropy and we present here the averaged values. The calculated spectra for γ-Al_2O_3 agree in general with the data for α-Al_2O_3. In this work we used a limited fragment of the γ-Al_2O_3 structure, which contains only octahedral cation vacancies.

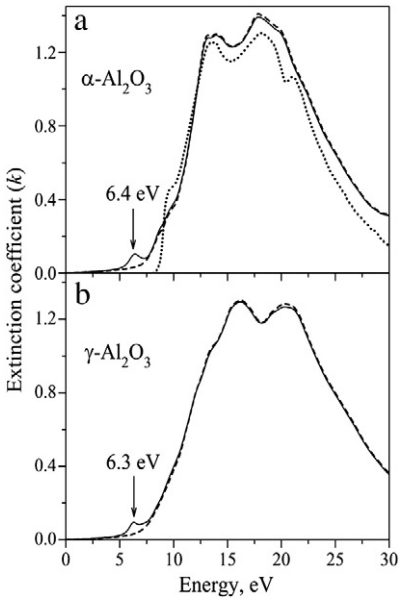

Fig. 2. Calculated extinction coefficient $k(h\nu)$ for α-Al_2O_3 (a) and γ-Al_2O_3 (b). Solid and dashed lines correspond to calculated spectra for alumina crystals with oxygen vacancies and for perfect alumina crystals, respectively; dotted line in the section above is an experimental spectrum for α-Al_2O_3.

The calculated spectra $k(h\nu)$ for the cells with oxygen vacancies in α- and γ-Al_2O_3 have peaks at 6.4 and 6.3 eV, respectively. They are absent in perfect crystals and can be related to oxygen vacancies. These energies are close to the experimentally obtained values for the absorption of F-centers in crystalline Al_2O_3[1–8]. This result supports the fact that the absorption peak 6 eV is related to oxygen vacancy.

3.2. Photoluminescence

For independent identification of oxygen vacancies we studied the low-temperature PL and PLE spectra of amorphous Al_2O_3 films. They are shown in Figs. 3 and 4, respectively. The same as in the case with crystalline Al_2O_3, the PL and PLE spectra of amorphous Al_2O_3 are a set of broad bands: a fine structure was not detected even at very low temperature (7.5 K). Thus, here the case of strong electron–photon interaction is realized and the Huang–Rhys values (S, average number of participating phonons) range from 9 to 12 [2,8]. In this case, the shape of the band is close to Gaussian.

In the PL spectra recorded at 6.52 eV excitation (Fig. 3), the slow component dominated by a wide 2.97 eV peak (with the full width at half maximum (FWHM) = 0.82 eV) followed by a weaker peak near 4.2 eV. The PL spectrum of fast component has the same peak at 2.97 eV, but predominant peaks are those close to 2.2 and 4.2 eV. The solid lines in

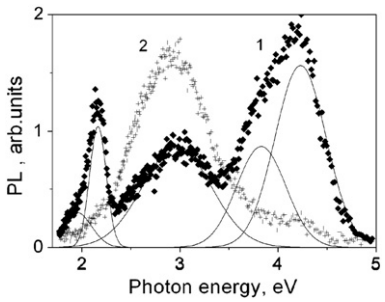

Fig. 3. Time-resolved PL spectra for amorphous Al_2O_3 film, obtained in the CVD process: 1, 2- fast and slow components, respectively. PL spectra were obtained at 6.26 eV excitation, T = 7.5 K. Points correspond to experimental spectra, solid lines show results of decomposition of spectrum 1 into Gaussian components.

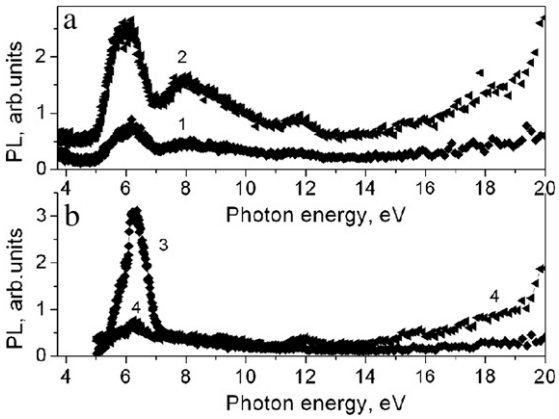

Fig. 4. Time-resolved PLE spectra for PL emissions at 2.9 (a) and 4.2 eV (b) in amorphous CVD Al_2O_3 films. (1, 3)- fast and (2, 4)- slow components. T = 7.5 K.

Fig. 3 show the Gaussian components into which the fast PL spectrum is decomposed. In addition to peak 2.97 eV, four additional peaks were detected: 1.95, 2.165, 3.83 and 4.23 eV with FWHM values 0.35, 0.2, 0.58 and 0.61 eV, respectively. The time-resolved PL spectra measurements evidence that the PL decay time is a few ns for the last four bands and is a few tens of ns for 2.97 eV. All these transitions were earlier observed in crystalline α-Al_2O_3 and are related to intrinsic defects formed during the growth, thermal treatment, and corpuscular irradiation rather than to impurities [1–8,27]. Thus, the slow band 3.0 eV with a low-energy shoulder in bulk α-Al_2O_3 is attributed to the occurrence of neutral oxygen vacancy (F-center) [2,8], whereas the fast band 3.8 eV is related to the same but positively charged center (F^+) [2,7]. Corresponding peaks were also observed in the spectra for amorphous Al_2O_3 films (Fig. 3): bands of F and F^+-centers have maximums at 2.97 and 3.83 eV, respectively. The low-energy bands 1.95 and 2.165 eV were observed at high irradiation doses and in strongly reduced Al_2O_3 crystals [27]. The bands 1.95 and 2.165 are assumed to be the result of some of pair defects (F_2 –centers). Another type of simple donor centers is interstitial cations. Optical transitions in Al^0, Al^+ and Al^{2+} range from 3 to 7.5 eV [27], but they are shifted to lower energies when these ions are incorporated into the Al_2O_3 structure.

The PLE spectra for 2.97 eV and 4.23 eV emissions recorded in time-resolved regime are shown in Fig. 4. In amorphous Al_2O_3 the 2.97 eV luminescence of F-centers is excited most efficiently in three ranges: 5–7, 7–10 and 18–26 eV. The PLE spectra recorded in time-resolved and time integrated regimes are similar to those for crystalline Al_2O_3[8,19]. The low-energy range corresponds to intra-center excitations in oxygen vacancy and the second is the excitation near the fundamental absorption edge ($h\nu \approx Eg$) and, finally, the increase in signal at $h\nu \geq 18$ eV demonstrates multiplication of electronic excitations at photon energy $h\nu \geq 2Eg$. It is well seen that the first range PLE spectra for 2.97 eV emission consists of two bands with maxima at approximately 5.7 and 6.3 eV (Fig. 4) and two maxima at 7.91 and 11.7 eV can be distinguished in the second range. The UV emission at 4.2 eV is best excited in the 6.31 eV band.

It is remarkable that the envelopes of PLE spectra for the emission of F-centers in amorphous Al_2O_3 film (Fig. 4) and in crystalline α-Al_2O_3[8] are rather similar. The main bands in the low-range for crystalline α-Al_2O_3 have maximums at 5.6 and 6.3 eV and the contribution of each depends significantly on the light polarization and sample orientation [8]. The intricate shape of the PLE spectrum for neutral oxygen vacancy results from the splitting of excited state in the crystal field of C_2 symmetry. In crystalline Al_2O_3 the 6.3 eV band has analogs in the photoconductivity [2] and exoemission [28]. This implies that the upper components of split excited state are localized in the conduction band and excitation in this band results in the ionization of oxygen vacancy and loss of an electron. Thus, the

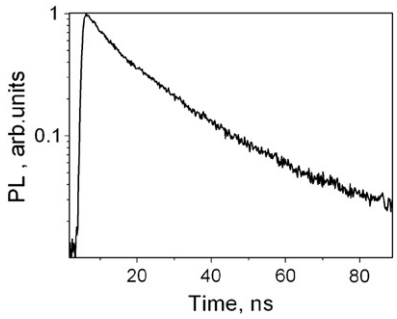

Fig. 5. PL decay for 4.2 eV emission at 6.26 eV excitation in amorphous Al_2O_3 film. T = 8 K.

luminescence at 2.97 eV and the 5.7 and 6.3 eV bands in the PLE spectra explicitly evidences the presence of neutral oxygen vacancies in amorphous Al_2O_3 films grown in the CVD process. The location of the PLE band close to 6 eV agrees well with the results of first principle quantum-chemical simulation in which the vacancy bands were found at 6.3 and 6.4 eV for α- and γ-Al_2O_3, respectively (Fig. 2). The presence of positively charged oxygen vacancies is inferred from the presence of 3.83 eV component in the PL spectra in Fig. 3.

The maximum of the second range PLE band is localized close to 9 eV for α-Al_2O_3[8], whereas for the amorphous Al_2O_3 film it shifts to 7.9 eV. As the features of this range are due to band-to-band transitions, this shift suggests that the forbidden band in the amorphous Al_2O_3 film is narrower than that in crystalline Al_2O_3.

Fig. 5 shows a decay for the low temperature 4.2 eV emission at 6.26 eV excitation. It is seen that the decay law differs considerably from exponential one: the decay curve is not a straight line in semi-logarithmic coordinates as in crystalline Al_2O_3[2–8]. The non-exponential character of the PL decay is, most likely, the result of direct tunnel recombination between ionized deep centers of luminescence and electrons captured in traps [29]. This, on the one hand, agrees with the data on photoconductivity and exoemission for Al_2O_3 and assumes ionization of deep centers at 6.26 eV excitation and, on the other, suggests the presence of a great amount of traps in amorphous Al_2O_3. The PL decay time during tunnel recombination depends on the distance between two interacting centers and in sum yields longer-term nonexponential decay in case of different distances between them [29]. It is very important to compare the concentration in amorphous and crystalline Al_2O_3 in direct experiments, for example, on thermostimulated luminescence and this work is being carried out.

4. Conclusions

In the PL spectra of amorphous CVD Al_2O_3 films we registered broad bands in the UV-to-visible spectral range. By analogy with crystalline Al_2O_3 the slow 2.9 eV PL excited in the band near 6.0 eV is related to the neutral oxygen vacancy. The identification of this PL band was supported by the results of first-principle quantum chemical simulation, which showed 6.3 and 6.4 eV bands in the extinction spectra for α- and γ-Al_2O_3, respectively. Other bands in the spectrum of PL fast component are attributed to ionized single vacancies (F^+-centers), divacancies (F_2) and, probably, interstitial Al.

Acknowledgment

The work was supported by integration grant No.70 from the Siberian Branch of the Russian Academy of Sciences.

References

[1] G.W. Arnold, D.W. Compton, Phys. Rev. Lett. 4 (1960) 66.
[2] B.G. Draeger, G.P. Summer, Phys. Rev. Lett. 19 (1979) 1172.
[3] P.W.M. Jacobs, E.A. Kotomin, Phys. Rev. Lett. 69 (1992) 1411.
[4] K.J. Caulfeld, R. Cooper, J.F. Boas, Phys. Rev. B Condens. Matter Phys. 47 (1993) 55.
[5] A. Stashans, E. Kotomin, J.-L. Galais, Phys. Rev. B Condens. Matter Phys. 49 (1994) 14854.
[6] Y.-N. Xu, Z.-Q. Gu, X.-F. Zhong, W.Y. Ching, Phys. Rev. B Condens. Matter Phys. 56 (1997) 7277.
[7] K. Matsunaga, T. Tanaka, T. Yamamoto, Y. Ikuhara, Phys. Rev. B Condens. Matter Phys. 68 (2003) 085110.
[8] A.I. Surdo, V.S. Kortov, V.A. Pustovarov, V. Yu. Yakovlev, Phys. Status Solidi. C 2 (2005) 527.
[9] A.I. Kingon, J.-P. Maria, S.K. Streiffer, Nature 406 (2000) 1032.
[10] J. Robertson, Eur. Phys. J. Appl. Phys. 28 (2004) 265.
[11] N. Novikov, V.A. Gritsenko, K.A. Nasyrov, Appl. Phys. Lett. 94 (2009) 222904.
[12] V.A. Gritsenko, K.A. Nasyrov, Yu. N. Novikov, A.L. Aseev, S.Y. Yoon, Lee Jo-Won, C.W. Kim, Solid State Electron. 47 (2003) 1651.
[13] C.-H. Cheng, J. Y.-M. Lee, Appl. Phys. Lett. 91 (2007) 192903.
[14] H. Nishikawa, R. Nakamura, Y. Ohki, Y. Hama, Phys. Rev. B Condens. Matter Phys. 48 (1993) 2968.
[15] C. Itoh, K. Tanimura, N. Itoh, M. Itoh, Phys. Rev. B Condens. Matter Phys. 39 (11) (1989) 183.
[16] H. Nishikawa, E. Watanabe, D. Ito, Phys. Rev. Lett. 72 (1994) 2101.
[17] S. Baroni, A. Dal Corso, S. Gironcoli, P. Giannozzi, C. Cavazzoni, G. Ballabio, S. Scandolo, G. Chiarotti, P. Focher, A. Pasquarello, K. Laasonen, A. Trave, R. Car, N. Marzari, A. Kokalj http://www.quantum-espresso.org/.
[18] M.C. Payne, M.P. Teter, D.C. Allan, T.A. Arias, Rev. Mod. Phys. 64 (1992) 4.
[19] G. Paglia, A.L. Rohl, C.E. Buckley, J.D. Gale, Phys. Rev. B Condens. Matter Phys. 71 (2005) 224115.
[20] E.M. Proupin, G. Gutierrez, Phys. Rev. B Condens. Matter Phys. 72 (2005) 035116.
[21] G. Gutierrez, A. Taga, B. Johansson, Phys. Rev. B Condens. Matter Phys. 65 (2001) 012101.
[22] H.P. Pinto, R.M. Nieminen, S.D. Elliott, Phys. Rev. B Condens. Matter Phys. 70 (2004) 125402.
[23] R. Ahuja, J.M. Osorio-Guillen, J. Souza de Almeida, B. Holm, W.Y. Ching, B. Johansson, J. Phys. Condens. Matter 16 (2004) 2891.
[24] C. Wolverton, K.C. Hass, Phys. Rev. B Condens. Matter Phys. 63 (2000) 024102.
[25] G. Zimmerer, Nucl. Instrum. Methods Phys. Res. Sect. A 308 (1991) 178.
[26] E.T. Arakawa, M.W. Williams, J. Phys. Chem. Solids 29 (1968) 735.
[27] M.J. Springis, J.A. Valbis, Phys. Status Solidi. B 123 (1984) 335.
[28] A.I. Surdo, V.S. Kortov, F.F. Sharafutdinov, Radiat. Prot. Dosim. 84 (1999) 261.
[29] V.N. Parmon, R.F. Khairutdinov, K.N. Zamaraev, Phys. Solid State 16 (1974) 2572.